

Ion beam transport from the source to the first orbits of a cyclotron

J.L. Belmont

I.S.N. 53 avenue des Martyrs F 38026 Grenoble cedex France

Abstract

The ions produced by an external source and axially injected into the cyclotron are considered. The ion beam, with a fit structure, must be carefully placed on the orbit to be accelerated and well extracted. One has to match: its position on the first turn, its shape, its chopped time structure due to radio frequency. A compromise between different necessities must be obtained. In fact beam losses can be significant, and the ion transfer efficiency from the source to the orbit varies from a few per cent to 70% !

Key words: axial injection, cyclotron

CONTENTS :

INTRODUCTION	3
HOW TO DESIGN THE ELEMENTS.....	4
THE LOW ENERGY BEAM TRANSPORT LINE.....	5
LENSES USED ALONG THE BEAM HANDLING	5
AN EXAMPLE OF LONG LINE : STUDIES OF A SEVERAL 100 M LONG LINE AT GRENOBLE.	6
ALIGNMENT OF THE OPTICS.....	7
SPACE CHARGE EFFECTS	8
VACUUM EFFECTS	9
CENTRAL REGION.....	11
RESEARCH OF THE CYCLOTRON ACCEPTANCE AND THE POSITION OF THE FIRST ORBIT....	11
INSIGHT INTO ORBIT CENTRING	12
<i>Effects of the accelerating gaps : centring</i>	12
<i>Effects of the accelerating gaps : focusing</i>	13
INFLECTORS	14
THE ELECTROSTATIC MIRROR	14
THE SPIRAL INFLECTOR	14
<i>To built the spiral inflector</i>	14

THE HYPERBOLOID INFLECTOR	14
EDGE EFFECTS AT THE INFLECTOR ENTRANCE AND EXIT	15
FOCUSING OF THE CYLINDRICALLY SYMMETRIC MAGNETIC LENSES.	15
THE BUNCHING	16
PERTURBATIONS OF THE BUNCHING	18
CODES	18
CONCLUSION.	18
ACKNOWLEDGEMENTS	19
REFERENCES	19
APPENDIX 1	21

Introduction

Probably more than one hundred years of man power has been spent throughout the world for solving the problems of ion axial injection [32] [6] [4] ! Different ways have been used, some methods are now obsolete but a large variety can be founded yet, depending on :

- ♦ The required transmission efficiency between the source and the target. The present tendency is to try to obtain good transfer : the ions can be very difficult to produce, like exotic isotopes, and cross sections of the nuclear reaction can be very small ! But in other cases, this efficiency is not the main problem.
- ♦ The efforts that one can put for the money and the man power and the quality of that man power : a very good efficiency between the source and the target postulate a lot of calculus, drawings, an array of equipments - but a simple design can give not too bad results !
- ♦ The flexibility of the machine to be matched to the different mechanical compromises necessary for the proposed solutions : noses of the accelerating dees, hole inside the yoke, level of magnetic field, room for the sources ... etc.

To extract a good quality beam from a cyclotron with a good yield implies that the internal beam is well controlled at its birth : the ions must be properly injected on their equilibrium orbit.

We describe briefly the different steps of axial injection devices.

1. The ions are extracted from the source held at the high voltage. After analysis from different kinds of extracted ions, the desired beam is made up, and its emittance calibrated. It is guided, more or less easily to the yoke. Each part of the guide must not only transmit the beam with its particular properties but also adapt this beam to the structure that follows. The beam must be matched to the conditions of the following part: it is the "matching" or adaptation of the emittances.

2. Inside the cyclotron yoke, the transport can use only the space available for optics, one has to take into account the reliability of the elements, the level of the vacuum, the magnetic fields created by the cyclotron.

3. The beam being at low energy, it takes little to perturb it : parasitic fields, out centring....

4. At the centre of the cyclotron an inflector bends the beam direction by 90° .

5. For each R.F. harmonic of the machine, one determines the beam shape, beam position and angle at the entrance of the first orbit, inflector and accelerating dee tips. One cannot choose an inflector and preceding guides without the previous knowledge of the central orbit !

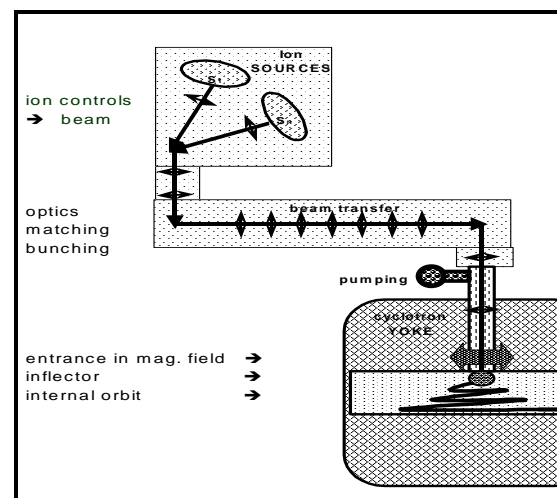


Figure 1. Diagram of axial injection

How to design the elements

If accurate field maps are available then the solution to all problems is the integration of the differential equations of the movement ... but with already known limit conditions! The configuration of the different electrodes and magnetic poles does not come from the solution of a set of “magic” equations ; it is rather the result of a great number of interactions between different parts of the injection system. For each kind of element one must choose an appropriate method of calculation. In addition, one must generally take into account the technology of fabrication, the space available, the time devoted for that and the price. This latter consideration has often been important!

The low energy beam transport line

The structure of the transfer from the source(s) to the cyclotron depends on the available space, the aim of injection, the desired quality and efficiency necessary for the extracted beam.

The ions are extracted from the source, analysed, the desired beam is made up, and emittances calibrated – figure 1. The transfer line may be from 1 or 2 meters long, until about 40 m if ion source is out of cyclotron cave. Several meter long line has to be used to match carefully the beam to the internal orbit, with corrections for chromatism, isochronism, stigmatism [29] [28] [3]. Very long line is now studied or is under construction with cascade of machines for radioactive ion beams [23] [16]; then a part of the line is only devoted to the simplest possible transport.

For each part, an appropriate method of calculation is chosen, taking into account the technology of fabrication, the space available, the time devoted for the studies, the construction, and price... This latter consideration has often been important. Inside the cyclotron yoke one pays special attention to the quality of the vacuum, the magnetic stray fields, the reliability of the elements, the “matching” of the emittances [27] [14]. The best way is to try to match the optics inside the 6 coordinates of phase space. For example at Ganil, for CIME, close to 7 meters are necessary and the decoupling between the 6 coordinates is obtained by specific sections included each one in each others.

The optics are built with magnets, electrostatic deflectors, and lenses like described in the table I and II .

Lenses used along the beam handling

Quadrupole	electrostatic ($\pm V_0$ on R_0)	magnetic ($nI_{(A.t.)}$ / pole R_0)
main advantages :	low cost	good vacuum efficient at high energy
Drawback :	a part is defocusing, astigmatic bulky, long outgazing wires and feedthrough aberrations	a part is defocusing astigmatic bulky, long power consumption large cost aberrations
focusing power \approx	$\propto (V_0 / V_{is}) (L/R_o^2)$	$\propto (nI / B\rho) (L/R_o^2)$
uses : for line, astigmatic matching, with magnets...	. Vancouver (40 m), . MSU (k500) . Texas (polarized I.S.)	. Ganil . Louvain . Dubna

TABLE I. Quadrupole lenses used along the low energy beam transport line.

Cylindrical Lens :	Einzel lens	solenoid lens ("Glaser" type)
main advantages :	<ul style="list-style-type: none"> ◆ low price ◆ compact, ◆ short 	<ul style="list-style-type: none"> ◆ focusing quality ◆ no degassing ◆ not disturbed by external field ◆ q/m dependent
Drawback :	<ul style="list-style-type: none"> ◆ aberrations (beam must be well centred) ◆ sparking 	<ul style="list-style-type: none"> ◆ heavy, large, expensive ◆ power consumption ◆ axis rotation : $\theta_{\text{rad}} = \{2B\rho\}^{-1} \int B(z) dz$
focusing power \approx	complicated formula !	$\propto \{(nI/B\rho)^2 L^{-1}\}$ $(nI_{(A.t.)}, \text{ for gap } \approx 3R_0)$
$\Phi_{\text{beam}}/\Phi_{\text{lens}} :$	$\ll 0.5$	< 1 (vacuum chamber)
uses : (- for line, - stigmatic matching)	<ul style="list-style-type: none"> ◆ for beam line : abandoned ◆ used at the exit of sources. (Ganil,...) 	<ul style="list-style-type: none"> ◆ used for beam line to : Berkeley, Catania (12), China, JAERI, Julich, JyvTMskyTM, MSU, South-Africa.... ◆ inside yoke : in all cyclotrons

TABLE II. Lenses with cylindrical symmetry used along the low energy beam transport line.

An example of long line : studies of a several 100 m long line at Grenoble.

In our institute we have studied a 120 m long line and experimented a such 18m FODO type line (focusing quadrupole, space, defocusing quadrupole, same space) [23] [14]

- ◆ The only equipment that was actually inside the beam tube ($\Phi=80$ mm) was beam position monitors, placed every 18 m. with ionic vacuum pumps.
- ◆ The periodic focusing structure was provided by ironless magnetic quadrupoles. Each quadrupole was 700 mm long and the distance between them was 800 mm, the pattern was 3 m long. These quadrupoles were in fact simply formed from copper bars connected in series, and through which a current of as much as 1500 A.(0.25 T/m) passes. The geometry provides a constant gradient, (better than $2 \cdot 10^{-3}$) upon 66% of the radius, 65 mm diameter.

The quadrupoles were mounted in groups of four, on 5.6 m long granite girders placed on adjustable jacks (like magnets of LEP, CERN). The alignment of the total assembly were achieved by means of these jacks, using a simple system of a stretched wire and a surveyor's level. This method (used on LEP) is simple and rapid : it could be repeated as often as necessary to compensate for ground subsidence. We have experimentally observed the importance of the rigidity of the granite which does not flow. A smooth oscillation of the axis, greater than the betatron wave length, here 20 m, is without any importance. Upstream a matching section 6 meter long was applied before the channel. Price of a such line is 4500 euros by meter, girders, diagnostics, pumps... all include... but without the building!

Alignment of the optics

It is well known that a beam must be centred in the lenses for reducing the aberration effects. However small positioning errors exist in the alignment of optical elements (figure 2), the diagnostics could also be off centred. External fields, like the **earth** magnetic field, or stray field from the main magnet of the cyclotron, particularly in the case of a superconducting one, can disturb the ideal trajectory. This way the real central trajectory snakes around a virtual axis which can in fact oscillate too, but with a period longer than the betatronic oscillation of the guide ! With correctors and monitors the machine operators must spent time to minimize the effects of these perturbations.

Stronger is the focusing effect of one lens (converging or diverging) stronger is the off centre displacement ; so the betatronic oscillation by pattern must be rather small and the number of lens as small as possible. For example, misalignments of regular FODO structure give less perturbations than with doublet or triplet periodical structures of quadrupoles, for the same admittance (but FODO requires a longer emittance matching section).

Example. About our 120m line, we have calculated the effect of misalignments. Our quadrupoles lenses, without iron, did not shield the earth magnetic field (external perturbation). The monitor was an oscillating wire. Note that an harp can change temporarily the potential well of the charges and so the effects of space charge and the beam envelope. The figure 3 shows 5 different positions of the central trajectory of the beam, obtained with 5 different sets of positioning errors of quadrupoles, stochastically disposed along the optics (for Rb^{1+} at 25 keV ; $B_p = 0.21 \text{ T.m}$; focus = $\pm 1 \text{ m}$; betatron oscillation of $\approx 50^\circ$ /pattern FODO))

- RMS value of quadrupole misalignments $\sigma = 0.3 \text{ mm}$ and 0.1 mrad
- first plane: without taking earth magnetic field into account
- and others, taking earth magnetic field into account ($0.7 \cdot 10^{-4} \text{ T.}$)

The sensibility to errors was minimal for a betatronic oscillation of 45° per pattern with control of the beam each 18 m. We note that the maximum acceptance of the actual guide is not for the theoretical value of $\approx 76^\circ$ /pattern without misalignment. A strong focalisation increases the beam angles due to the positioning errors, and a too small one does not keep the beam along the theoretical axis !

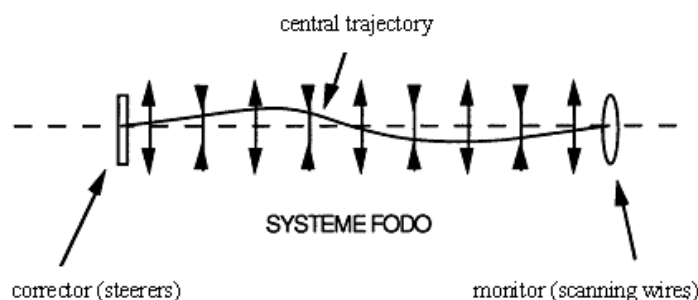


Figure 2. Central trajectory of the beam along stochastically disposed optics with one control of the beam position.

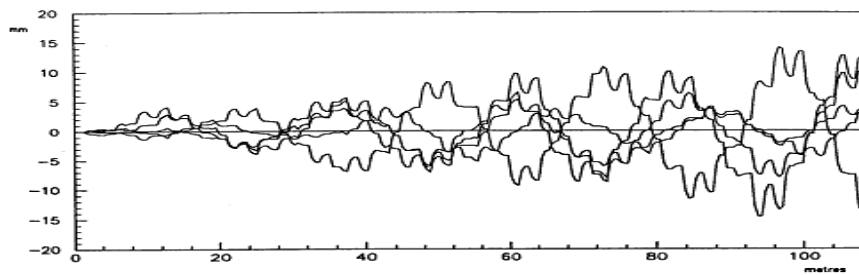
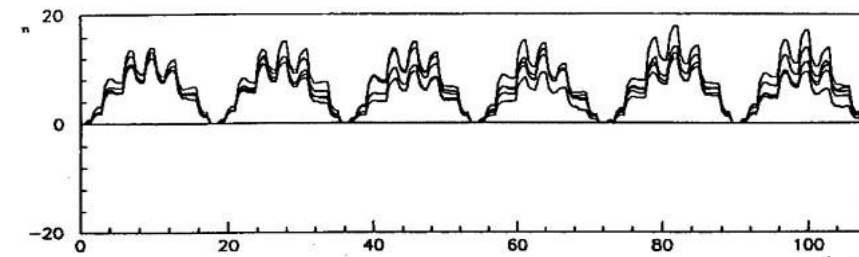
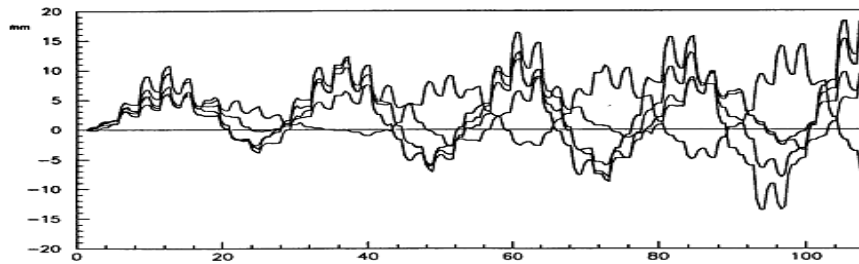
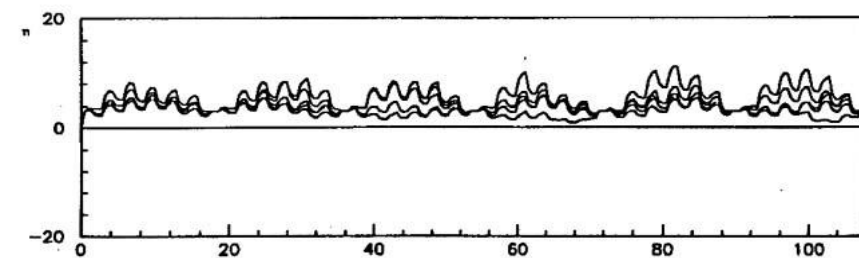


figure 1. trajectoires sans champ magnétique terrestre



With corrections each 18 m (12 quadrupoles) and earth magnetic field



With corrections each 18 m and effects of earth magnetic field corrected by a systematic off-centering

Figure 3. 5 different positions of the central trajectory of the beam, obtained with 5 different sets of positioning errors of 72 quadrupoles, stochastically disposed along the optics, without and with control of the beam each 18 m (12 quadrupoles).

Space charge effects

For an high beam intensity, or even for medium intensity of high charged heavy ions, one has to consider the space charge effects. The very useful differential equations proposed by Lapostolle and Sacherer [33] describe the beam envelopes and are included in the code "Transport" of CERN, PSI at Villigen, and others... This code is easy to use, but some times it does not well describe the reality because of a neutralization of charges by capture of electrons or ions. To keep the validity of calculus, some laboratories eliminate theses effects with electrodes sweeping up the secondary charged particles. The adjustment of the optics must be made on pulsed beam at full intensity. The emittance, due to damage by the space charge, increase with the square of the run distance [14].

For having an *insight* into these phenomena, let suppose a revolution symmetry envelop beam, with intensity I_0 , a radius E , emittance $\pi\epsilon$, accelerated by the high voltage V to the velocity $v = \beta c$: the differential equation is : (with : $Z_0 = (4\pi\epsilon_0 c)^{-1} = 30 \text{ Ohm}$)

$$E'' + k(s) E - (\epsilon^2 / E^3) - I_0 (Z_0 / \beta) (1 / (V E)) = 0$$

Thus approximately, a beam line with an average focusing k (average focalisation of k . m per meter) keeps its diameter when the current increases from zero to ΔI , if we also increase k to $k + \Delta k$. One finds the relative increase of k : (the smaller is this variation than k and $V^{3/2}$ is the larger)

$$\frac{\Delta k}{k} = \Delta I \frac{Z_0}{\beta} \frac{1}{V \epsilon \sqrt{k}}$$

For example: let a small current of Ar^{6+} accelerated by $V = 10 \text{ kVolts}$, $\epsilon = 80 \text{ mm.mrad}$, focused by lens with average focus per meter $f = 1.7 \text{ m}$ (betatronic phase progression per meter: 45°), for keeping the same beam diameter with $10 \mu\text{A}$ one finds that the focus must decrease from 1.7 m to 1.35 m .

The difference of potential between beam axis and the vacuum chamber wall of radius R_0 , for a beam of uniform density, is :

$$V_a = I_0 (Z_0 / \beta) \{1 + \text{Log} (R_0 / E)\}$$

In the preceding example, the potential well of Ar^{6+} is $V_a = 0.45 \text{ Volts}$ for $(R_0 / E) = 5$. That well potential is sufficient for gathering the secondary electrons.

To decrease the space charge effects, a solution is to increase the focusing per meter (even by reducing the beam diameter like into RFQ). A better solution is to increase the ion source high voltage V : the emittance decreases like $V^{-1/2}$, the limited current and the variation of k (versus the intensity) like $V^{3/2}$. We note that with a high voltage V the beam is less perturbed by external magnetic fields and the focusing of the beam during the first turns inside the machine is less depending on the RF phase (see later). Inconvenient : design, cost, sparks, difficult use of cylindrical lenses, power consumption, high voltage of R.F. dee for clearing the centre... As a result of that, Ganil rebuilt axial injection with $V = 100 \text{ kV}$ (1992), Agor injects with $V = 40 \text{ kV}$ and Triumf with $V = 288 \text{ kV}$. At Julich, $V < 8.5 \text{ kV}$ is very small value for the present use of the machine.

At several hundred kilovolts, like for PSI [38] axial injection of the 72 MeV injector, problems and designs are different that those exposed here, nevertheless it is an expensive but very good solution!

Vacuum effects

The residual gas along the trajectory has 2 main effects on the beam: lost of ions (the most important) and emittance increase.

For a ion of charge q , in a gas “target” with a first potential of ionisation J , the cross section σ of the charge exchange from q to $q-1$ is given with a good approximation by A. Schlachter [37] :

$$\sigma_{q,q-1} = 1.43 \cdot 10^{-12} q^{1.17} J^{2.76} \text{ cm}^2$$

The transmission T through a tube L meter long, with a known residual gas (influence of $J^{-2.76}$) at the pressure P is: (one can neglected the other transformations that $q, q-1$)

$$T = e^{-(C\sigma LP)} \quad \text{with } C = 2.65 \cdot 10^{22} \text{ (m}^2\cdot\text{m.mbar)}^{-1}$$

For example we have tested the transmission of Rb^{1+} on the 18 m FODO line, depending on the nature of residual gas and its pressure. As we measured σ is practically independent of the energy (measures from 3 to 30 keV). One has the following transmission through 18 m. The pressure P of the injected gas is measured in the middle of 18 m tube, one small ionic pump at each end, and the tube having been outgassed several day at 200°C leading to negligible effect of the outgassing of our wall chamber. (P in mbar, 1 mbar = 100Pa):

$$\text{with nitrogen : } T = e^{-19100.P} ; \quad \text{with argon } T = e^{-20060.P} ;$$

$$\text{with xenon : } T = e^{-38700.P} ; \quad \text{with helium } T = e^{-2390.P} .$$

These measures give the σ values about 2 times smaller than from Schlachter's equation. (not so bad for a such cross section !)

In a project of ion transfer with $q = 15+$ along 60 m we should need a vacuum $P = 2.5 \cdot 10^{-8}$ mbar: it is important that the design of the beam line take that pressure into account.

The H^- are often used with axial injection, precisely for avoiding lost of accelerated H^- inside the cyclotron, lost due to the important gas leak by an internal ion source.[17]. If H^- is transported inside a 18 meters long channel with nitrogen residual gas, we should have $T = e^{-78000.P}$

The emittances increase linearly with the pressure and depends on the nature of the residual gas and a few on the structure of the optics. At the pressure where the charge exchange is small, this effect is *negligible*. For example Rb^{+1} inside a nitrogen pressure $2 \cdot 10^{-5}$ mbar, the emittance increase is 9π mm.mrad (measured and calculated), but it is zero below the necessary 10^{-6} mbar for a good transmission.

Central region

Research of the cyclotron acceptance and the position of the first orbit

The beam must reach the plane of symmetry of the machine in a precise position and the beam emittance must be adjusted to the structure of the cyclotron. For that, the emittance of the beam accelerated by the cyclotron has to be known in order to prepare it upstream.

Central region designs for various accelerating systems have been described extensively in the literature. The ways for obtaining these orbits are in very large numbers, from the simple use of a compass for a rotation in constant magnetic field to the most sophisticated codes of the integration of the movements due to fields, themselves either measured or calculated with (huge) codes.[7]

For the determination of that central region design the general process is approximately the following

- 1) One must find a stable central orbit and its eigen emittance for the central R.F. phase of the burst accelerated, a little far from the centre, orbit witch corresponds to a good extraction (calculus of “accelerated equilibrium orbit”). Then, one calculates (or estimates !) the backward trajectory and emittance through the dee tips to the entrance inside the first accelerating gap. It is the location where the beam, which arrive from 90° inflector with its previous energy, must be injected. One finds a central point for injection (S) and a correlated centre of curvature (Ω). (fig 4). At that point one seeks how is the actual beam which can be realised and injected in fact, then one calculates forward this set of particles and one checks if it is well accelerated [29]. Note that generally the position of the centre of rotation Ω depends on the R.F. phase : for that reason the phase range cannot be large!
- 3) One defines a real inflector satisfying the preceding conditions. The beam must be injected centred on the hole yoke axis : (see figure 4, axis at the point O, with its centre of curvature Ω and radius of curvature R_m , the inflector exit at the point S)
- 4) The upstream optics, throughout the yoke and the inflector, should provide the relevant beam like it has been previously calculated. This emittance depends on the R.F. phase too: a perfect matching to a large phase range is impossible.
- 5) It is necessary to do a lot of iterations for adapting the designs, specially the design of dee tips and eventually that of the inflector.

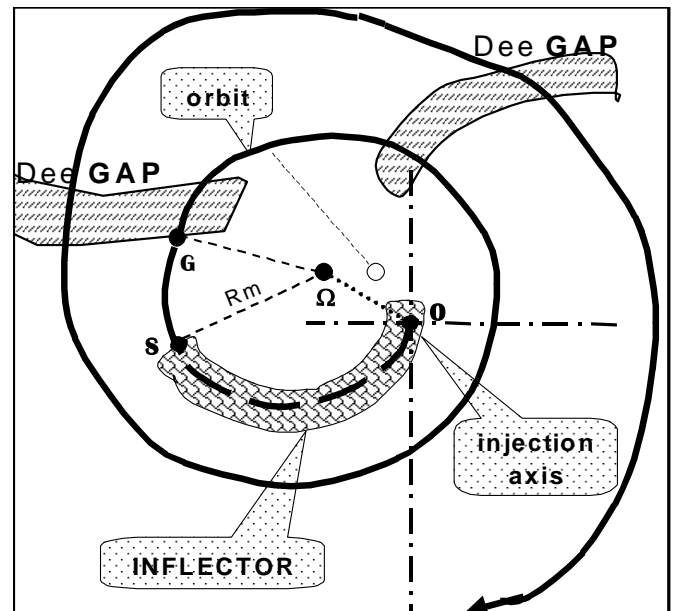


Figure 4. Artistic view of the projection of the central orbit at the injection inside a cyclotron.

6) For each RF harmonics, the technical structures are to be found, mainly the shapes of dee tips and of inflectors. These devices must not interfere! The beam path is normally operated in constant orbit mode for a given harmonic mode, i.e. the ions follow the same trajectories: the charge q , mass m , the source to V volts, the magnetic field level B following the law :

$$(mV)/(qB^2) = \text{cte}$$

V and V_{RF} must be proportional too.

Insight into orbit centring

At each iteration of calculations one proposes to change something and it is interesting to save time and to foresee qualitatively the effects of the proposed change. It is a very large time consuming task to calculate all the fields with accuracies and to compute the movements due to the forces.

Effects of the accelerating gaps : centring

If an accelerating interval of width d has an electric field E (it is the “hard edge” approximation on an interval d , with a constant magnetic field) like:

$$E = E_0 \sin \varphi \quad \text{with } E_0 \text{ constant and } \varphi = (\omega t + \varphi_0)$$

φ_0 is the initial phase at the entrance inside d , at the time $t = 0$.

The equation of motion can be integrated *analytically* to yield a simple relationship between the initial values of magnetic radius $R_m = R_0$, α_{in} , φ_0 , $t=0$ and the final ones R_s , α_{out} , φ_s , t_s . (see figure 5). One finds that the centre of curvature is displaced *perpendicularly to E_0* by

$$\Delta Y_c = (R_0/2dh) \{ \sin(\Delta\varphi + \varphi_0) - \sin\varphi_0 \} \quad \Delta\varphi = h \omega_{ion} t_s$$

with $\Delta\varphi = h \omega_{ion} t_s$ and $h = R.F.$ harmonic versus ions, generally not integer here (bump or well of magnetic field in the centre, the magnetic field is not exactly isochronous, and one takes this into account by the relation : $\omega_{R.F.} = h \cdot \omega_{ion} = h \cdot qB/m$).

ΔY_c depends largely on the R.F. phase φ_0 at the entrance.

α_{in} is the angle at the gap entrance between the vector of velocity and the normal to the 2 parallel equipotentials and α_{out} the angle at the gap exit.

For simple, for fast (and fairly precise) calculations, each successive first gap has to be decomposed into 11 to 21 successive hard edge equipotential surfaces (supposed parallel 2 by 2) and for each of the 10 or 20 small different gaps the above hard-edge calculus are applied. Now these equipotentials are obtained by numerical code. Each gap (decomposed in 10 to 20 small gaps) can be moved independently in one piece, very quickly by a small code (without looking for the equipotentials, the gap keeping the same form). In this way the shape of the dee tips are found easily. (See Grenoble, Nice, Agor, Crakow ...)[18] [35] [36]. This way, several tens of layout can be tested in a morning !

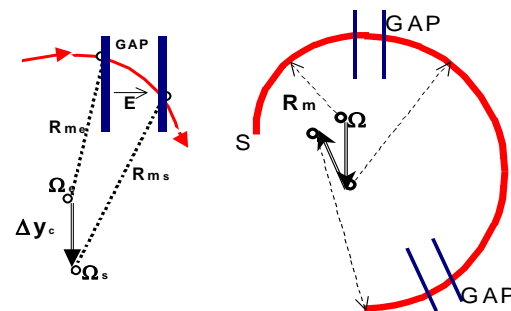


Figure 5. Effect of one or several accelerating intervals with an electric R.F. field E .

The example of orbit centres of the Grenoble cyclotron is shown figure 6 for $h = 2$. Orbits are depending on initial phase. The 21 equipotentials have been measured in a rehographic tank and they were fitted with parabola, easy to use!

Note that, now, the tracking codes of the ion trajectories inside the calculated field maps are may be accurate and fast enough !

Effects of the accelerating gaps : focusing

The electrical vertical focusing due to the crossing of the accelerating gaps has to be calculated (at least for example, vertical components of electric fields can be obtained by development in series of Maxwell laws, close to the median plan). Unfortunately in the centre the magnetic field is not vertically focusing. The convergence (or divergence !) properties vary with the RF phase. Like we have seen, particles are not necessarily isochronous : one can choose the injection phases which correspond to a converging effect by the first gaps (with a graduated phase shift of the accelerated bunch to the central accelerated phase of the orbit at a larger radius).

The presence of posts (or rods) crossing the median plane changes the focusing. Roughly, without vertical post the vertical focusing is twice more efficient, compensating the lack of magnetic focusing. Indeed without post the electric field extends deeply inside the dee and the dummy dee, like that, during the gap crossing, the phase shift is more important than with posts and the horizontal focusing is zero (it is without steering effect).

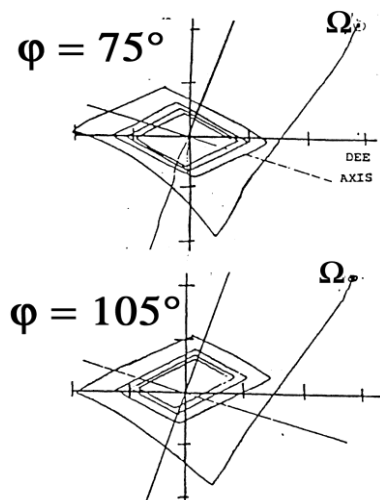


Figure 6. An example of orbit centres depending on initial R.F. phase inside the Grenoble Cyclotron

Beam centring is easier with several posts, but the different orbits of the several RF harmonics in a such close space, leads to limit the number of posts.

The variations of these centrings and the vertical focusing, depending on RF phases, decrease with the energy injection.

The global apparent emittances (horizontal and vertical) of the internal beam, which mixes the emittance resulting from a phase mixture, will be larger and larger when the phase width of the bunch increases (but in fact the history of extracted trajectories and there oscillations depends on the RF phases too).

Inflectors

Now, if we know *where* to inject the beam, we must choose one of the three types of inflectors (and their parameters) for bending the beam into the median plane. We have to satisfy the position of the inflector exit (point S), the centre of rotation at this exit (Ω) and the magnetic radius R_m ; later we will have to match the emittances of the beam arriving through this inflector.

The electrostatic mirror

The device consists essentially of a pair of planar electrodes which are positioned at an angle of about 45 degrees to the incoming ion beam [21] [15]. The upper electrode is formed by a grid of fine wires. The ions enter the electric field of the mirror obliquely and lose some of their kinetic energy; they are then reaccelerated in the desired direction by the same electric field. The electrostatic mirror is attractive from the standpoint of simplicity and its reduced volume; it is not limited to work at constant orbit unlike the 2 others types of inflector. Its main disadvantages are that the applied potentials must be of the same order of magnitude as the ion source potential (sparks), its indispensable grid is destroyed by the high currents of heavy ions, and at its exit there is a restricted choice for the position of the centre Ω . Its use is mainly reserved for cyclotron with only one active dee like at Berkeley (roughly, in that case Ω is on the gap, the locus of oscillations of the rotation centres). The focusing and the coupling of vertical and horizontal motions are both weak. The effective emittance at its exit is slightly increased as compared to the source emittance and a part of the current is absorbed by the grids that one has to change from time to time.

The spiral inflector

The spiral inflector (also named “Belmont-Pabot inflector”) (figure 7) would be a cylindrical deflector in absence of a magnetic field (and the central trajectory would be inside a vertical plane) but in presence of the axial magnetic field B_z , this plane rotates as the particles gain radial velocity [31]. The central trajectory belongs to an hyperboloid. The shape and length of this inflector are determined by the parameter $K_0 = A/2R_m$, where A is the *electric* radius and R_m the *magnetic* radius in a field B_z . The height of the inflector is A . The figure 7 shows, as a function of the parameter K_0 , a set of normalized (to R_m) trajectories projections in the median plane and the loci of corresponding orbit centres at the exit (loci of the point Ω). The electric field is directed along the X-axis at the entrance. Its magnitude remains constant throughout the whole inflector. The central trajectory is at constant energy and the deflection effect of electric field is maximum : this inflector is compact, without grid, and has a sophisticated shape.

To obtain a more flexible design, a radial electric field component, proportional to the magnetic force along the trajectory, may be introduced. Such an electric field is obtained by gradually tilting the electrode surfaces and decreasing the gap. It is “*a spiral inflector with slanted electrodes*”. In this way, an adjustable shift of the orbit centre at the exit is obtained, for a given K_0 value. The loci of Ω are large, it is not a line but a surface. Its characteristic parameter is : $k_0 = \tan \psi_s$, where ψ_s is the slant of electrodes with respect to the horizontal plane at the *exit* of the inflector. Its versatility has to be paid by its beam acceptance often smaller than without slant and by an increased complication of the machining procedure because of the continuously varying gap requirement.

. Generally the equations of motion are given in function of K , with : $K = K_0 + (k_0/2)$. (See appendix 1)

The differential equations of this spiral inflectors are very coupled and must be numerically integrated [6] [31] [1] (see appendix 1). The obtained transfer matrix is very coupled and leads to difficult matching. The apparent emittances, in X , X' and Y , Y' planes, increase. It is the price of its compactness... The acceptance depends on parameters, it is quite large ; at Grenoble it was more than 400π mm mrad, with a 8 mm gap width) [2]

To built the spiral inflector

To draw the mechanical piece (made of copper-beryllium) is sophisticated. It is no evident to find a volume to put in the 2 insulators ; depending on cyclotrons, solutions are various ! Calculus and drawing made (one has to determine the lathe part, and milling machine part, and the position of reference axis) the machining is relatively simple ! One can cut the electrodes like spirals by successive holes with a milling machine. At Grenoble, 20 years ago, without automatic machine like we can have now, in less than half a day, we carved out the ramp, by drilling of 120 holes with the translatory and rotation motions calculated for each hole !

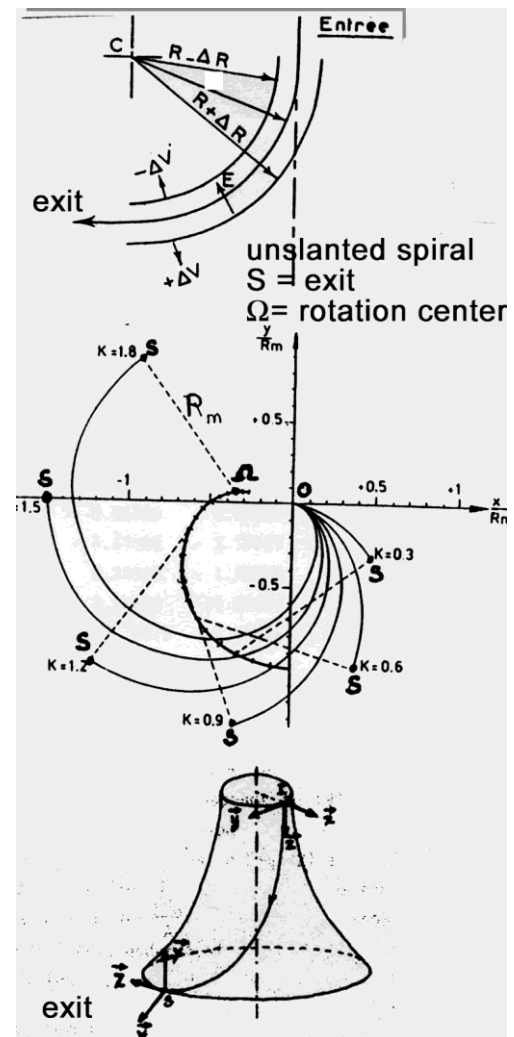


Figure 7. The spiral inflector. Projections of the trajectories and Ω , depending on K_0 , on the median plane. The central trajectory belongs to an hyperboloid

The inflector must be *carefully isolated* from high R.F electric field. The 1 mm thick shielding of the Grenoble inflector is close to 1.5 mm from the inflector where the electric field is perpendicular to the magnetic field. It has been easily built by electrolytic depositing of copper on aluminium (sophisticated and precise) shape like the inflector, after that copper depositing the aluminium was chemically dissolved.

The hyperboloid inflector

The electrodes are formed by two pieces of concentric hyperboloids and their rotation axis is parallel to the magnetic field (figure 8). From the beginning to the end of the trajectory the beam rotation is 20.2° . The central trajectory is along an equipotential, but the contribution of electric field is not always to bent by 90° the beam. This inflector is not compact. The distance between the rotation centre Ω and the injection axis "O" is $1.74 R_m$ and this axis is necessarily different from the axis of symmetry of the cyclotron : one have to drill the hole inside the yoke at that position which is in fair condition only *without* any magnetic saturation [36]. There are no free parameters for the adjustment of the position of the point Ω .

The differential equations of these inflectors are analytically solved [22] [15], the analytic transfer matrix for the transfer of the 6 dimensions of a beam is decoupled for a particular choice of the axis of reference : that hyperbolic inflector allows to construct easily an optics of *good quality*. It is used inside Julic and Ganil cyclotrons.

Edge effects at the inflector entrance and exit

On these two last types of inflector few millimetres of the electrodes are cut out (shortened) to eliminate the expansion of electric fringing field at its ends [41]. At Grenoble we have cut 4.5° of inflection ($4.5^\circ/90^\circ$) at each sides of inflector.

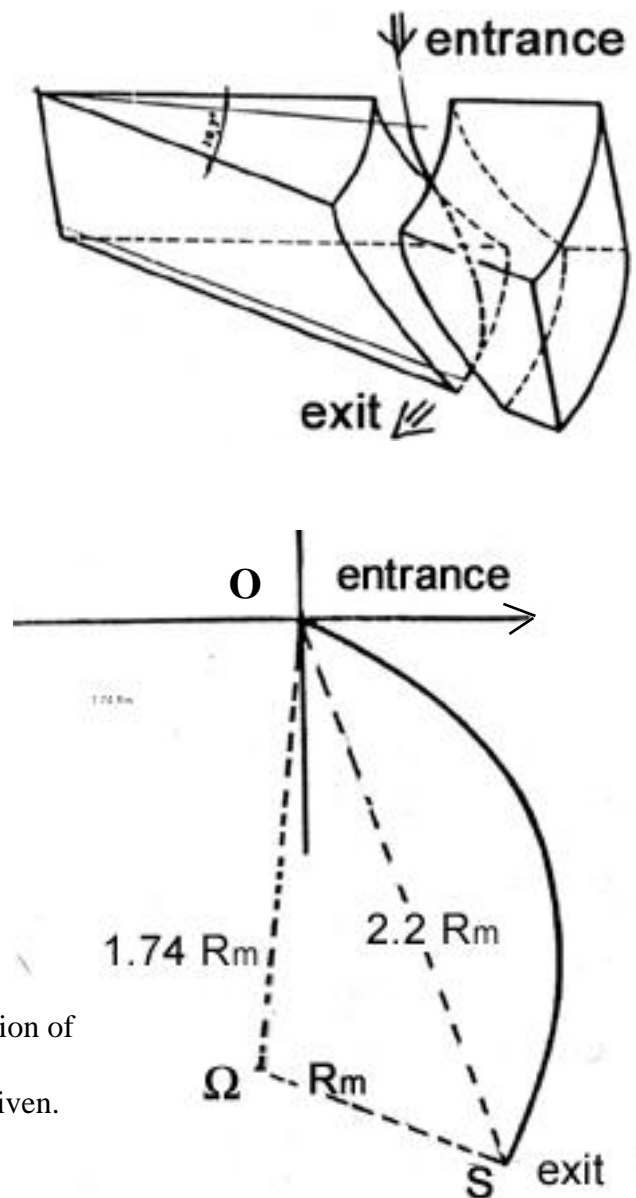


Figure 8. The hyperboloid inflector. Projection of the trajectory. on median plane. For a given magnetic radius R_m , the triangle $O S \Omega$ is given.

Focusing of the cylindrically symmetric magnetic lenses

Whatever the inflector, a coupling is given by the magnetic field inside the yoke, along the beam injection but like for the magnetic Glaser lenses decoupling is obtained, here, by a rotation of axis. When the beam arrives from part without field and enters inside the field it crosses radial components B_r of magnetic lines (figure 9), giving to the ion velocity a component of rotation proportional to B_r and B_r is proportional to the distance r from the axis of symmetry :

$$B_r = -\frac{r}{2} \left(\frac{\partial B_z}{\partial z} \right) + \frac{r^3}{16} \left(\frac{\partial^3 B_z}{\partial z^3} \right) + \dots$$

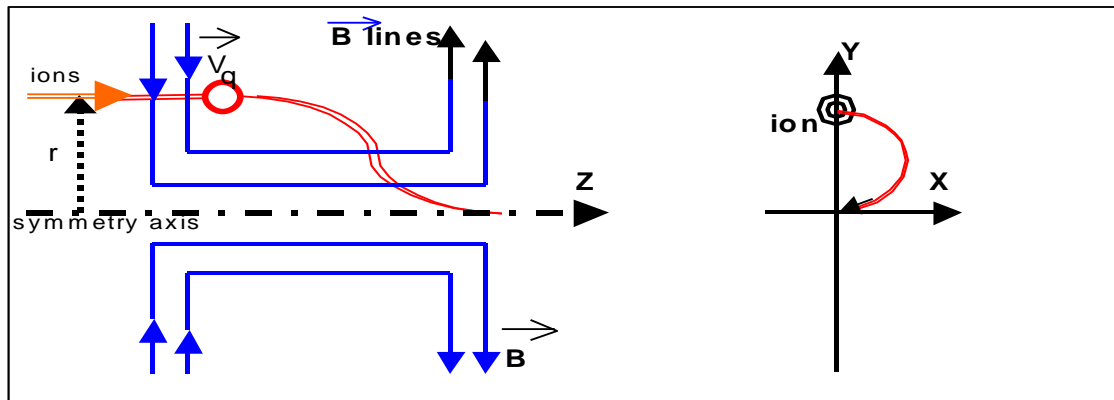


Figure 9. When the beam arrives from part without field and enters inside the field it crosses radial components B_r of magnetic lines, giving to the ion velocity a component of rotation.

The effect of axial field on this component leads to a rotation of the beam and a focusing (the diameter is r in the hard edge approximation). At the field exit the rotation stops (see Glaser lenses). We understand :

- 1) We must inject the beam axis centred on the symmetry axis of the magnetic field.
- 2) The beam always arrives inside the inflector with that velocity of rotation (which continues inside the inflector, but effects included inside equations).
- 3) The lengths of the paths and the velocities along the axis and for a particle at the radius “ r ” from the beam axis are different : the lens is not isochronous (see farther the effect on the “bunching” in case of a long path like inside superconducting cyclotron yokes).

In hard edge approximation, for a path l long with h the R.F harmonic, one has:

$$\Delta l \approx \frac{l}{8} \frac{r^2}{Rm^2} \quad \text{or} \quad \Delta \Phi^\circ \approx 7.2 \frac{r^2}{Rm^3} lh$$

- 4) At the reverse, the ions of ECR sources are created inside a magnetic field (and in that case, they are not inside a rotating plane) and at the *exit* of that field they *receive* a radial component of the velocity. This phenomena is the origin of the (apparent) large emittance of that type of source [19] and leads to an other kind of coupling that one attempts to reduce for example with the help of the axial magnetic field of the yoke.

The bunching

The source produces a continuous beam.[42] [12] In the last part of the transfer line, the “bunching” is set : by modulating the beam velocity during the RF period, more particles can be squeezed inside the phase range of the RF in which the ions are correctly accelerated (figure 10). We have seen above, several times, the advantages of a narrow R.F. phase width for increasing the quality of the extracted beam..

The idea is to decelerate particles in advance relatively to a central particle and to accelerate particles late relatively to that central particle. Farther from the inflector this effect is

applied, smaller is the acceleration-deceleration to apply. To group all the ions inside a narrow width of RF phase should impose to apply a *linear* velocity variation to ions.

To apply a such sawtooth variation of the velocity is more difficult to realize than to use a simple sine variation which is “linear” during only a small part of the period !

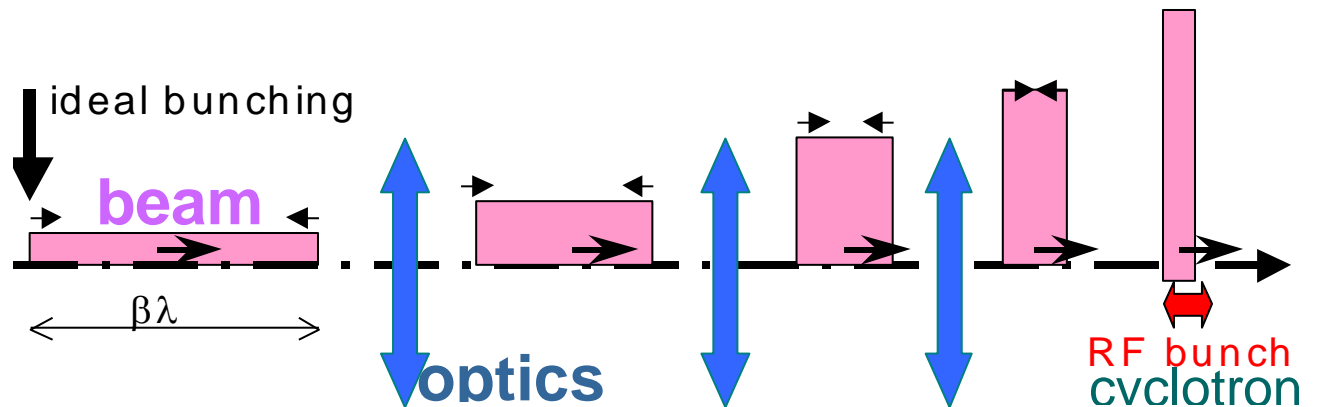


Figure 10. Artistic view of the bunching ! (density of particles in Y-axis)

Several axial injection systems employ a sine wave R.F. “buncher” and so the intensity of the extracted beam increases by a factor 3 to 5. The buncher is a simple tube, close to $\beta\lambda/2$ long, ($\beta = v/c$ and $\lambda = \lambda_{RF}$) on which several hundred volts R.F. are applied (with an adjustable phase) (figure 11).

To go closer the sawtooth one uses R.F. harmonics ! (intensity gain 8 to 15). Several tubes apply the different harmonics. A distance between tubes is equivalent to have more harmonics [14].

An interesting solution is the use of a single gap with two grids between which an electric field, close of the sawtooth, is applied (figure 12). At the entrance inside the central device of the buncher, the width of the first gap is adjusted to $\beta\lambda$ and has no effect [12]

An other proposed solution is to apply parabola voltage on a tube : that produces a sawtooth energy variation, but electronics are not easy to built ! [11]

At the bunching corresponds an energy spread and for a very good quality of the accelerated beam one needs chromatic optics and even partially isochronous ones. That is provided by the external line like previously indicated. In this case, the bunching must be applied

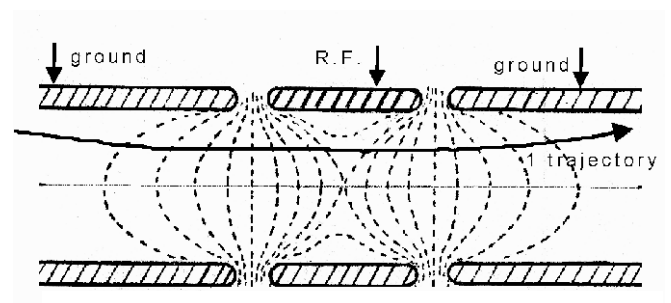


Figure 11. Equipotentials due to the R.F. applied. Their integrated effects depend on the ion positions inside the “inflating”.

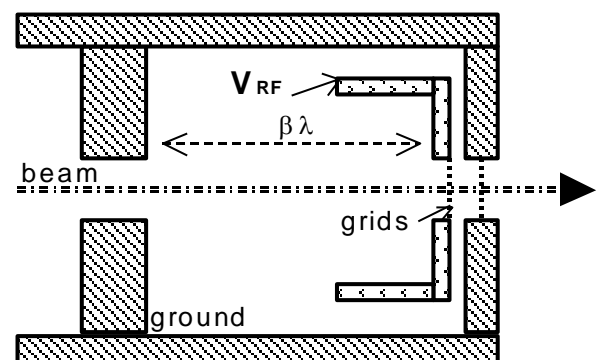


Figure 12. Single gap buncher for the sawtooth signals

far from the centre (like Cime of Ganil), this way one has the space for applying the different functions to the optics (and its problems of construction, setting and centring!). It is the opposed solution with a significant space charge or for the supraconducting cyclotrons: the bunching must be applied as close as possible to the inflector, with a high variation of velocity.

Perturbations of the bunching

We saw the necessary linearity of the velocity variation that is disturbed by the energy spread of the ion source, the instability of the power supply of acceleration, the space charge, the “inflating” of the equipotentials crossed not at the same position along the buncher tube, depending on the radius of the ion (see fig.11). One minimises this last effect by using a small diameter for the tube, requiring a beam waist, often slightly gridded (at Grenoble with only one thin ribbon on the diameter of the extremity of each tube). The longitudinal space charge effects are cured by positioning the buncher close to the inflector, the repulsing between ions compensating itself the energy spread at the inflector level with a proper combination of buncher voltage and the DC beam current”[40].

As indicated earlier (see fig.9), due to the different path lengths inside the magnetic field, the supra conducting cyclotrons or saturated iron cyclotrons encounter difficulties to bunch : again it is better to bunch as close as possible to the inflector if, this way, the path after the buncher along the magnetic field is reduced. But then the drawback of chromatic effect of the inflector appears. Here like along the optics, it is always particles “far” from the centre of the emittance that are lost !

For example the gain of Catania cyclotron bunching is about 4 ; this way the efficiency of injection reaches 36%.

Codes

A lot of very confident codes are written, and available (unhappily not always very well exportable!). Note : LIONS (orbits), GALOPR and SOSO (space charge, bunching, trajectory), CHA3D (map) at Ganil/Caen [7]; and RELAX3D (maps), CASINO (inflector), SPUNCH (bunching) at Triumf/Vancouver, TRANSPORT (beam), POISCR (map) at CERN etc..

Conclusion.

The choice of devices results from compromises taking into account : *the feasible* implementations on the actual machine, *the accuracy* of the known field maps in one’s possession, *the time* assigned to the task. These choices will depend upon the different *means of the laboratory* : financial, calculation, conception and realisations. To build an axial injection is always a challenge! Now one can have the help of the lot of studies which have been done on the subject all over the world. Roughly, if the number of dee is the same, centres are not very different or are homothetic : that can help to start a project. The adaptation of the beam to the cyclotron centres is a difficult part. Nevertheless, whatever the relentlessness to find solutions, generally one cannot solve all the problems for all R.F. harmonics : the cyclotron users have to choose the main range of energy and to limit the diversity of particles to be accelerated. For example at Grenoble we abandoned the use of 1st RF harmonic, interfering with the neutron production.

Depending upon the designs, the ion transfer efficiencies, from the head of the beam transfer to the internal orbit, vary from a few per cent up to 70%. Common values are rather 10% to 20%.

Acknowledgements

The author would like to acknowledge the help of people who supplied information for this paper.

References

- [1] Baartman R., *The spiral inflector* int. rep. Triumf D.N. 90-32
- [2] Balden et al, *Aspect of phase space* 12th Int. Cyc. Conf. p.435
- [3] Bashevov V.V. et al. *Simulation of the transmission* 16th Int. Cyc. Conf. p.387
- [4] Bellomo G. *The central region for compact cyclotrons* 12th Int. Cyc. Conf. p.325
Bellomo G. *Axial injection project for the Milan sup. cyclo.* 11th Int. Cyc. Conf. p.503
- [6] Belmont J.L. & Pabot J.L.. IEEE Trans. NS-13 p.191 (1966)
Belmont J.L. et al., *Axial injection and central region of AVF cyclotrons*
ISN Internal report ISN-86-106 (From: Lecture notes of 1986
RCNP KIKUCHI summer school, RCNP Osaka University) and :
ISN (now : "LPSC") Internal report ISN-86-106 (1986)

Ion transport from the source to the first cyclotron orbit
NUKLEONIKA 2003;48(Supplement 2):S13-S20
- [7] Bertrand P. *SPIRAL facility at Ganil : ion beam simulation...* 15th Int. Cyc. Conf. p.458
Bertrand P. *Inflecteur de Pabot-Belmont* GANIL Int. Rep. PB 38-87
- [8] Bertrand P. et al, *Specific correlations under space charge* 16th Int. Cyc. Conf. p.379
- [9] Bourgarel M.P. et al. *Modification of the Ganil injection* 12th Int. Cyc. Conf. p.111
- [10] Bourgarel MP. et al. *Ganil axial injection design* 12th Int. Cyc. Conf. p.161
- [11] Brautigam W. *H- operation of the cyclotron* 15th Int. Cyc. Conf. P 654
- [12] Chabert A. et al, *The linear buncher of SPIRAL* . N.I. and M. A 423 p.7
- [13] Clark D.J. et al. *Berkeley 88-inch cyclotron* 5th Int. Cyc. Conf. p.610 and 11th Int. Cyc. Conf p.499
- [14] De Conto J.M., *R.I.B. at Grenoble : beam transport and acceleration* 4th EPAC
- [15] Hazewindus N. W. *axial injection system* N.I. and M. 96 p.227
Hazewindus N. *The axial injection system of the SIN injector cyclotron* N.I. and M. 129 p.325-340
- [16] Heikkinen P. et al. *Ion optics in the Jyväskylä K130 cyclotron* 13th Int. Cyc. Conf. p.392
- [17] Heikkinen P., et al, *Feasibility studies of H- acceleration* 15th Int. Cyc. Conf. p.650
- [18] Khallouf A. *"Trajectoires centrales"* Thesis I.S.N - Grenoble (1986)
- [19] Krauss-Vogt W. *Emittance and matching of ECR sources* N.I. and M. A 268
- [20] Linch F.Y. et al, *Beam buncher for heavy ions* N.I. and M. 159 p.245
- [21] Marti F. et al. *Axial injection in the K500 super. cyclo.* 11th Int. Cyc. Conf. p.484

- [22] Müller R.W. *Novel inflector for cyclic accelerators* N.I.M.; 54; p.29
- [23] Nibart V., *Transport d'ions exotiques* Thesis Grenoble I.S.N. Inter. report. ISN-96-01
- [25] Pabot J.L. *Contribution à l'étude de l'I.A.* Thesis 1968 CEA report R-3729
- [26] Pandit V.S. et al. *Modification of a double drift beam bunching* 16th Int. Cyc. Conf.
- [27] Ricaud Ch. et al. *Status of the new high intensity injection system* 2nd EPAC p.1252
- [28] Ricaud Ch., *Commissioning of the new high intensity A.I.* 13th Int. Cyc. Conf. p.446
- [29] Ricaud Ch., et al. *Preliminary design of a new H. I. injection and 6-dimentional beam matching for axial injection* 12th Int. Cyc. Conf. p. 372 and p. 432
- [30] Rifuggiato D. et al *Axial injection in the LNS super. cyclo.* 15th Int. Cyc. Conf. p.646
- [31] Root L., *Design of an inflector for Triumf cyclotron* Thesis
- [32] Ryckewaert G. *Axial injection systems for cyclotrons* 9th Int. Cyc. Conf. p.241
- [33] Sacherer F.J., IEEE Trans. NS-18 p.1105 (1971)
- [35] Schapira J.P. *Agor central region design* 12th Int. Cyc. Conf. p.335
- [36] Schapira J.P. & Mandrion P., *Axial injection in the Orsay super. cyclo.* 10th Int. Cyc. Conf. p.332
- [37] Schlachter A. *Charge change collisions* 10th Int. Cyc. Conf. p.
- [38] Schryber U. et al. *Status report on the new injector at SIN* 10th Int. Cyc. Conf. p.43
- [39] Skorka S.J IEEE Trans. NS 28 - p.129
- [40] Stambach Th. et al.; *The PSI 2mA beam and future applications* 16th Int. Cyc. Conf.
- [41] Toprek D. *Beam orbit simulation in the central region* N.I. and M. A 425 p.409 (1999)
- [42] Weiss M., *Bunching of proton* 13 IEEE NS 20 p.877 & IEEE NS 20 13 p.800 (1972)

Appendix 1

Equations concerning the “spiral” or “Belmont-Pabot” inflectors

The z axis is the axis of axial injection parallel to the (constant) magnetic field , x-y plane is in the median plane.

A is the electric radius of curvature, the height of the inflector ; (at the exit, in the median plane of cyclotron, $z = -A$), R_m is the magnetic radius of the first cyclotron orbit.

The ion path length s along the axis is given by $s = A\theta$

$K = A/2R_m$ - but with slanted electrodes with an angle ψ ($\tan \psi = \tan \psi_s * \sin \theta$) with ψ_s at the exit of the inflector , one have to take : $K = A/2R_m + (\tan \psi_s)/2$

Central trajectories are given by :

$$x = -\frac{A}{2} \left[\frac{2}{4K^2 - 1} + \frac{\cos(2K+1)\theta}{(2K+1)} - \frac{\cos(2K-1)\theta}{(2K-1)} \right]$$

$$y = \frac{A}{2} \left[-\frac{\sin(2K+1)\theta}{(2K+1)} + \frac{\sin(2K-1)\theta}{(2K-1)} \right]$$

$$z = -A(\sin \theta - 1)$$

The differential equations of the trajectories near to the central one were established by

J.L.Pabot and completed by L.Root .

α, β, γ are the Freynet's coordinates along the central trajectory given above, with **A** the unit on length. α has the electric field direction at the entrance of the inflector.

“ ’ ” means $d/d(s/A) = d/d\theta$. α', β', γ' for the initial conditions are coupled by the entrance inside the magnetic field

$$\begin{aligned} \alpha'' = & + \alpha \left[1 + \frac{1 + 2 k_0 k' \sin^2 \theta}{1 + k_0^2 \sin^2 \theta} + 2k' k_0 \cos^2 \theta \right] \\ & + \beta k_0 \sin \theta \left[\frac{1 + 2 k_0 k' \sin^2 \theta}{1 + k_0^2 \sin^2 \theta} \right] + \beta' (2k' + k_0) \cos \theta \\ & - 2\gamma' \\ \beta'' = & + \alpha \left[k_0 \sin \theta \frac{1 + 2 k_0 k' \sin^2 \theta}{1 + k_0^2 \sin^2 \theta} + (2k' + k_0) \sin \theta \right] \\ & - \alpha' (2k' + k_0) \cos \theta \\ & + \beta [2k_0 k' + k_0^2 \sin^2 \theta \frac{1 + 2 k_0 k' \sin^2 \theta}{1 + k_0^2 \sin^2 \theta}] \\ & - \gamma' (2k' + k_0) \sin \theta \\ \gamma'' = & + 2\alpha k_0 k' \sin \theta \cos \theta + 2\alpha' \\ & + \beta (2k' + k_0) \cos \theta + \beta' (2k' + k_0) \sin \theta \\ & - \gamma k_0^2 \sin^2 \theta \end{aligned}$$

